

Beyond Homophily: Structure-aware Path Aggregation Graph Neural Network

Yifei Sun¹, Haoran Deng¹, Yang Yang^{1*}, Chunping Wang², Jiarong Xu³,
Renhong Huang¹, Linfeng Cao¹, Yang Wang² and Lei Chen²

¹College of Computer Science and Technology, Zhejiang University

²Finvolution Group

³Department of Information Management and Business Intelligence, Fudan University

{yifeisun, denghaoran, yangya, renh2}@zju.edu.cn, jiarongxu@fudan.edu.cn,
{wangchunping02, wangyang09, chenlei04}@xinye.com, linfengcao1996@gmail.com

IJCAI 2022

Code:None

2022. 09. 07 • ChongQing



gesis
Leibniz-Institut
für Sozialwissenschaften



Reported by Chenghong Li

Introduction

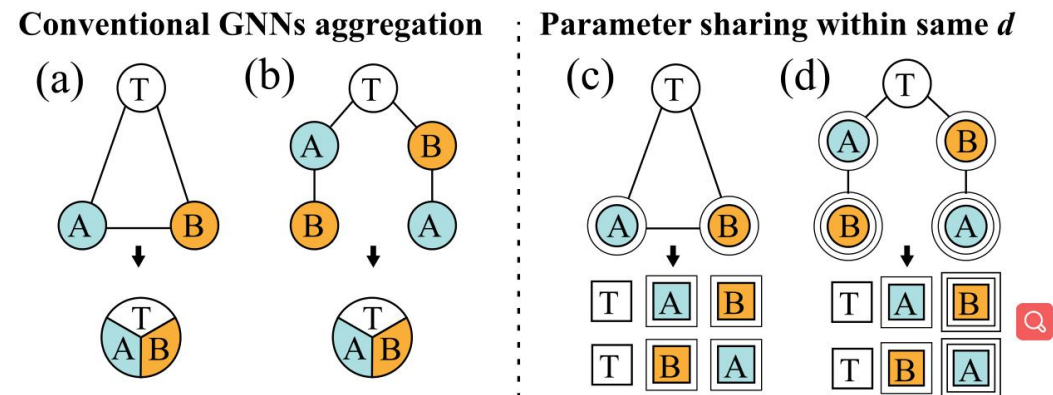
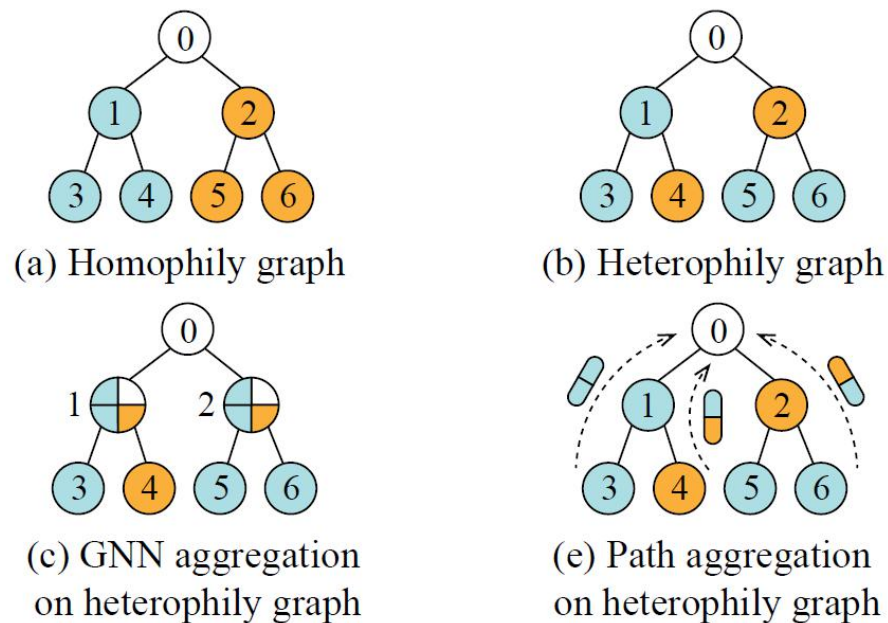


Figure 3: Intuitive case where GNNs are not able to distinguish the target nodes in (a) & (b), while our path-based aggregation with parameter sharing mechanism can capture the topological information and make the embedding distinguishable (c) & (d). (Nodes with similar characteristic represented as the same notation.)

Figure 1: (a) & (b) show patterns of homophily and heterophily graphs. (c) demonstrates the GNN aggregation process for node 0 of (b). (d) our proposed path aggregation compared with (c).

Method

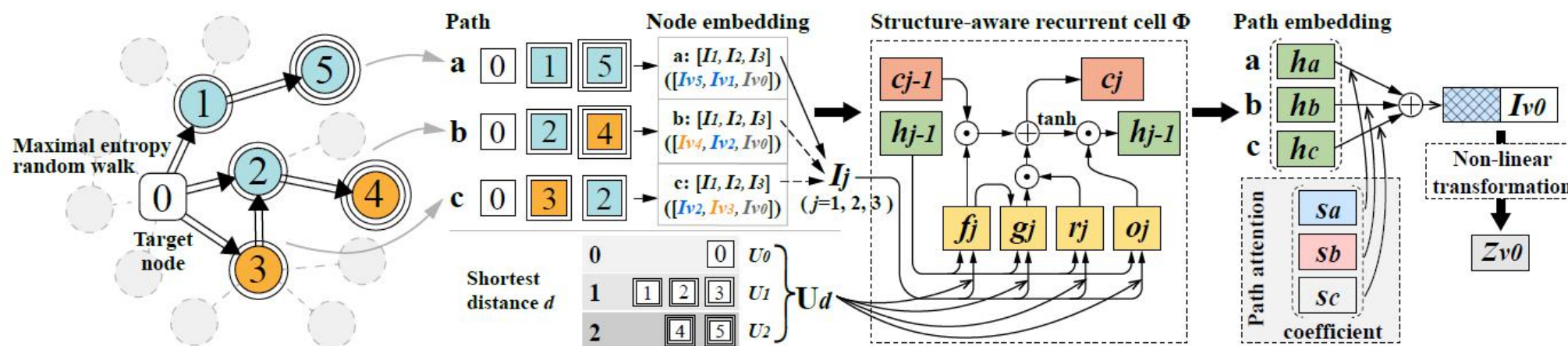


Figure 2: The workflow of PathNet for node classification of node 0 with the walk length $k = 3$. The color of node stands for label and the number stands for node index.

Method

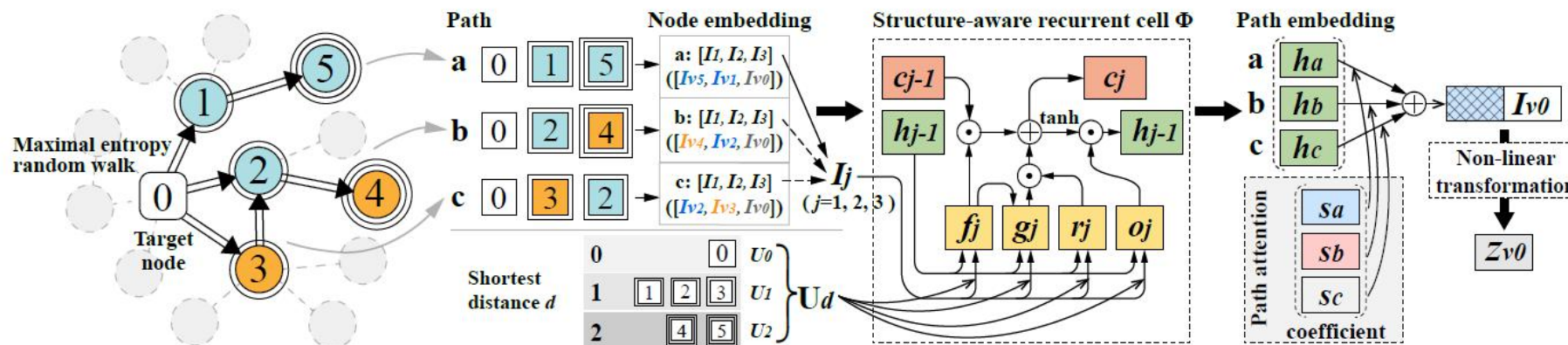


Figure 2: The workflow of PathNet for node classification of node 0 with the walk length $k = 3$. The color of node stands for label and the number stands for node index.

$$\eta = - \sum_i \pi_i \sum_j p_{ij} \ln p_{ij}. \quad (1)$$

$$\mathbf{P}_u = \frac{\mathbf{D}_u^{-1} \mathbf{A} \mathbf{D}_u}{\lambda}, \quad (2)$$

Method

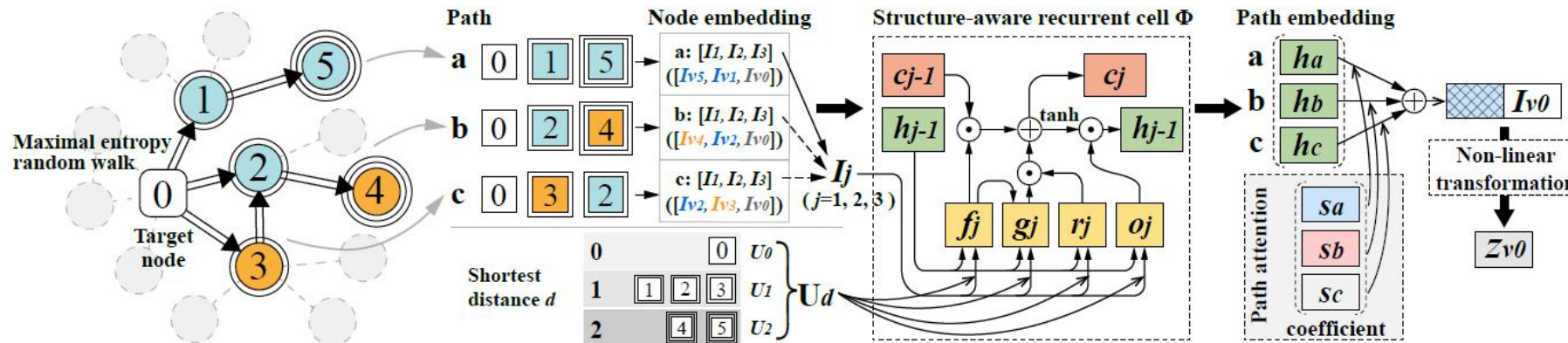


Figure 2: The workflow of PathNet for node classification of node 0 with the walk length $k = 3$. The color of node stands for label and the number stands for node index.

$$\mathbf{I} = \sigma(\mathbf{W}_{\text{in}}\mathbf{X} + \mathbf{b}_{\text{in}}), \quad (3)$$

$$\mathbf{s}_{v,p} = \text{SOFTMAX}(\delta(\mathbf{a}(\mathbf{I}_v \parallel \mathbf{h}_p))), \quad (5)$$

$$\begin{aligned} \mathbf{r}_j &= \sigma(\mathbf{W}_{\mathbf{r}} \cdot h_{j-1} + \mathbf{U}_{\mathbf{d}} \cdot \mathbf{I}_j), \\ \mathbf{f}_j &= \sigma(\mathbf{W}_{\mathbf{f}} \cdot h_{j-1} + \mathbf{U}_{\mathbf{d}} \cdot \mathbf{I}_j), \\ \mathbf{o}_j &= \sigma(\mathbf{W}_{\mathbf{o}} \cdot h_{j-1} + \mathbf{U}_{\mathbf{d}} \cdot \mathbf{I}_j), \\ \mathbf{g}_j &= \tanh(\mathbf{W}_{\mathbf{g}} \cdot h_{j-1} + \mathbf{U}_{\mathbf{d}} \cdot \mathbf{I}_j), \\ \mathbf{c}_j &= \mathbf{f}_j \odot \mathbf{c}_{j-1} + \mathbf{r}_j \odot \mathbf{g}_j, \\ \mathbf{h}_j &= \mathbf{o}_j \odot \tanh(\mathbf{c}_j), \end{aligned} \quad (4)$$

$$\mathbf{z}_v = \sigma\left(\mathbf{W}_{\text{out}}\left(\mathbf{I}_v \parallel \sum_{j \in p} \mathbf{s}_{v,p} \mathbf{h}_p\right) + \mathbf{b}_{\text{out}}\right). \quad (6)$$

Experiments

| | | Cora | Pubmed | Citeseer | Cornell | NBA | BGP | Electronics |
|-------------|--------------|-------------------|-------------------|-------------------|-------------------|-------------------|-------------------|-------------------|
| #Hom. ratio | | 0.81 | 0.80 | 0.74 | 0.30 | 0.39 | 0.37 | 0.25 |
| Baselines | MLP | 74.75±2.22 | 86.65±0.35 | 72.41±2.18 | 81.08±6.37 | 59.21±6.92 | 63.39±0.34 | 75.03±0.08 |
| | GIN | 84.97±1.51 | 86.97±0.53 | 72.19±1.74 | 58.10±5.70 | 65.47±6.85 | OOM | OOM |
| | GAT | 82.68±1.80 | 84.68±0.44 | 75.46±1.72 | 58.92±3.32 | 67.19±1.04 | 62.25±0.90 | 64.64±0.27 |
| | GraphSage | 86.90±1.04 | 88.45±0.50 | 76.04±1.30 | 75.95±5.01 | 61.70±2.40 | 61.71±0.85 | 74.92±0.19 |
| | MixHop | 85.41±1.61 | 86.38±0.46 | 75.43±1.89 | 72.51±6.36 | 68.89±5.95 | 64.80±0.83 | 67.84±0.50 |
| | H2GCN | 86.21±0.98 | 87.86±0.19 | 76.73±1.48 | 81.27±4.63 | 66.67±7.02 | 65.13±1.01 | 73.92±0.52 |
| | GPRGNN | 86.00±2.46 | 86.56±0.29 | 78.45±0.27 | 50.82±3.28 | 48.25±4.97 | 61.49±0.40 | 75.79±0.16 |
| | FAGCN | 86.30±1.74 | 88.50±0.27 | 76.20±1.45 | 72.70±4.50 | 63.49±3.89 | 64.48±0.55 | 71.10±2.02 |
| | P-GNN | 68.05±1.30 | 84.97±0.38 | 64.81±1.29 | 58.65±3.21 | 58.41±7.40 | 54.04±3.81 | 57.25±2.78 |
| | GeniePath | 85.15±0.65 | 86.50±0.34 | 76.46±1.42 | 59.19±4.43 | 68.73±5.41 | 63.15±2.94 | 73.39±0.35 |
| SPAGAN | 86.12±0.54 | 85.10±0.19 | 77.41±0.82 | 55.41±2.18 | 53.65±7.23 | 52.59±0.67 | 53.93±5.08 | |
| Ablation | PathNet-MLP | 82.89±2.84 | 87.86±0.07 | 75.78±1.50 | 90.54±1.35 | 69.05±6.08 | 64.36±0.54 | 75.81±0.58 |
| | PathNet-GRU | 84.76±1.52 | 87.89±0.12 | 76.57±1.08 | 90.74±1.81 | 69.52±7.16 | 64.46±0.76 | 76.16±0.52 |
| | PathNet-LSTM | 84.39±2.77 | 87.89±0.14 | 76.44±2.86 | 91.35±1.62 | 69.37±6.27 | 65.19±0.79 | 76.12±0.39 |
| | RW-PathNet | 85.08±1.17 | 87.84±0.34 | 78.54±2.13 | 90.27±2.16 | 71.27±5.65 | 64.92±0.61 | 76.31±0.45 |
| | PathNet-Mean | 83.46±2.36 | 88.18±3.94 | 76.59±1.61 | 91.08±2.43 | 70.16±6.18 | 64.81±0.77 | 76.85±0.55 |
| | PathNet-Sum | 84.21±1.43 | 86.93±0.27 | 74.80±2.44 | 89.19±2.70 | 67.70±6.44 | 65.39±0.83 | 75.06±0.44 |
| | PathNet | 85.76±2.67 | 88.92±0.21 | 77.98±2.40 | 91.35±2.91 | 71.69±4.83 | 65.72±0.66 | 76.97±0.84 |

Table 1: Mean accuracy and standard deviation of PathNet on node classification compared with baselines and ablation study.

Experiments

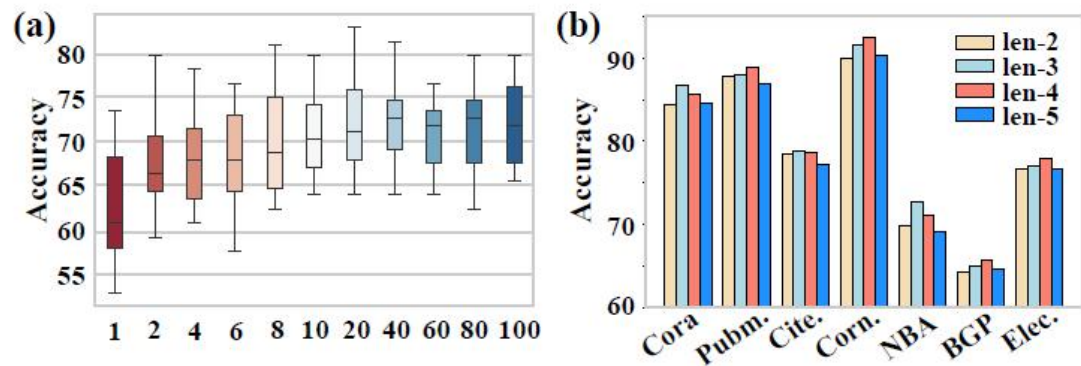


Figure 4: Model variants of different number (a) and length (b) of sampled paths.

| | Syn-Cora | Syn-Citeseer |
|-----------------------------|-------------------|-------------------|
| #Hom. ratio \mathcal{H}_G | 0.37 | 0.39 |
| GIN | 51.40±1.55 | 59.09±2.71 |
| GAT | 36.96±1.60 | 47.44±1.76 |
| GPRGNN | 43.62±1.69 | 53.95±1.87 |
| PathNet | 57.59±1.54 | 71.42±1.15 |

Table 2: Node classification on synthetic datasets.



Thanks